Colloid and Interface Science Communications 56 (2023) 100737

Contents lists available at ScienceDirect

Colloid and Interface Science Communications

journal homepage: www.elsevier.com/locate/colcom

Rapid Communication

Large-scale synthesis of CISe/ZnS core-shell quantum dots and its effects on the enzymatic activity of recombinant human furin (an activator of SARS-COV-2 S_1/S_2 spike proteins)

Vuyelwa Ncapayi [a,b], Oladoyin Famutimi [c], Thabang Calvin Lebepe [a,b], Rodney Maluleke [a,b], Sam Masha [a,b], Nande Mgedle [a,b], Sundararajan Parani [a,b], Tetsuya Kodama [d], Isaac Olusanjo Adewale [c,**], Oluwatobi Samuel Oluwafemi [a,b,*]

[a] Department of Chemical Sciences (Formerly Applied Chemistry), University of Johannesburg, Doornfotein 2028, South Africa
[b] Centre for Nanomaterials Science Research, University of Johannesburg, P. O. Box 17011, Doornfontein, 2028 Johannesburg, South Africa.
[c] Department of Biochemistry and Molecular Biology, Obafemi Awolowo University, Ile-Ife, Nigeria
[d] Department of Biomedical Engineering, Graduate School of Biomedical Engineering, Tohoku University, 4-1 Seiryo-machi, Aoba-ku, Sendai 980-8575, Japan

ARTICLE INFO

Keywords:
Furin
Quantum dots
Enzyme inhibitor

ABSTRACT

We herein report, for the first time, the activity of copper indium selenide/zinc sulphide core-shell quantum dots (CISe/ZnS QDs) as an inhibitor against recombinant human furin, an enzyme that has been implicated in the aetiology of many diseases, including Covid-19. The cell viability of the as-synthesised CISe/ZnS QDs was tested against mouse colon carcinoma cells (C26), while the Furin activity was measured by hydrolysis of peptide substrate Pyr-RTKR-AMC liberating the fluorogenic 7-amino-4-methyl coumarin. The result showed that the as-synthesised stable near-infrared emitting (840 nm) CISe-ZnS QDs is biocompatible against C26 and can inhibit furin with an inhibition constant, K_i, of 15.66 μM. The IC_{50} was 11.29 ± 0.54 μM, while the enzymatic activity was abolished at about 23 μM of the inhibitor concentration. The results indicate the chemotherapeutic potential of CISe-ZnS QDs as an enzyme inhibitor, which may find application in managing diseases whose pathogenesis involves hyperactivity of furin.

1. Introduction

Proprotein convertases are a group of serine proteases with diverse functions in mammals. Their name derives from the fact that they act by activating other proteins. The human genome encodes hundreds of proteases which play vital roles in the maintenance of body physiology and homeostasis [1]. They have evolved over thousands of years and thus have similarities with lower organisms hence the name proprotein convertase subtilisin/kexin type (PCSKs) [2]. There are at least nine families of PCSKs. One member of the family, PCSK3, EC. 3.4.21.75, also called furin (derived from feline sarcoma oncogene upstream region gene) and PACE (paired basic amino acid cleaving enzyme) has attracted a lot of attention recently because its expression has been reported to be upregulated in many human diseases. Increased furin enzymatic activity has been observed in atherosclerosis, head and neck cancer, lung, brain and skin tumours, among others [3,4]. It has also been implicated in bacterial and viral entry mechanisms into the host cell. In the case of SARS-COV-2, furin is reported to be involved in activating the S_1/S_2 spike proteins, thus enhancing viral entry into the host cells [5]. Therefore, furin inhibitors have been reported as promising therapeutic agents for diseases related to furin activities. Peptide or protein inhibitors are usually not attractive as drugs because of their large size, immunogenicity, in vivo instability, and low cell permeability among other disadvantages. Therefore, low molecular weight non-peptide inhibitors with high metabolic and proteolytic stability, known structure, and ease of synthesis are needed as better alternatives [6].

Luminescent ternary I–III–VI QDs ($CuInS_2$, $AgInS_2$, $CuInSe_2$ and $AgInSe_2$) quantum dots are emerging as promising candidates and alternatives for Cd-based QDs in biological applications [7–10]. Their intrinsic photostability, Fourier Transform Emission Transfer (FRET), long fluorescence lifetime properties and reduced toxicity have made them an ideal material for diverse applications ranging from biological

* Corresponding author at: Department of Chemical Sciences, University of Johannesburg, P. O. Box 17011, Doornfontein, 2028 Johannesburg, South Africa.
** Corresponding author.
E-mail addresses: kodama@tohoku.ac.jp (T. Kodama), olusanjo2002@yahoo.co.uk (I.O. Adewale), oluwafemi.oluwatobi@gmail.com (O.S. Oluwafemi).

https://doi.org/10.1016/j.colcom.2023.100737
Received 23 April 2023; Received in revised form 1 August 2023; Accepted 2 August 2023
Available online 5 August 2023

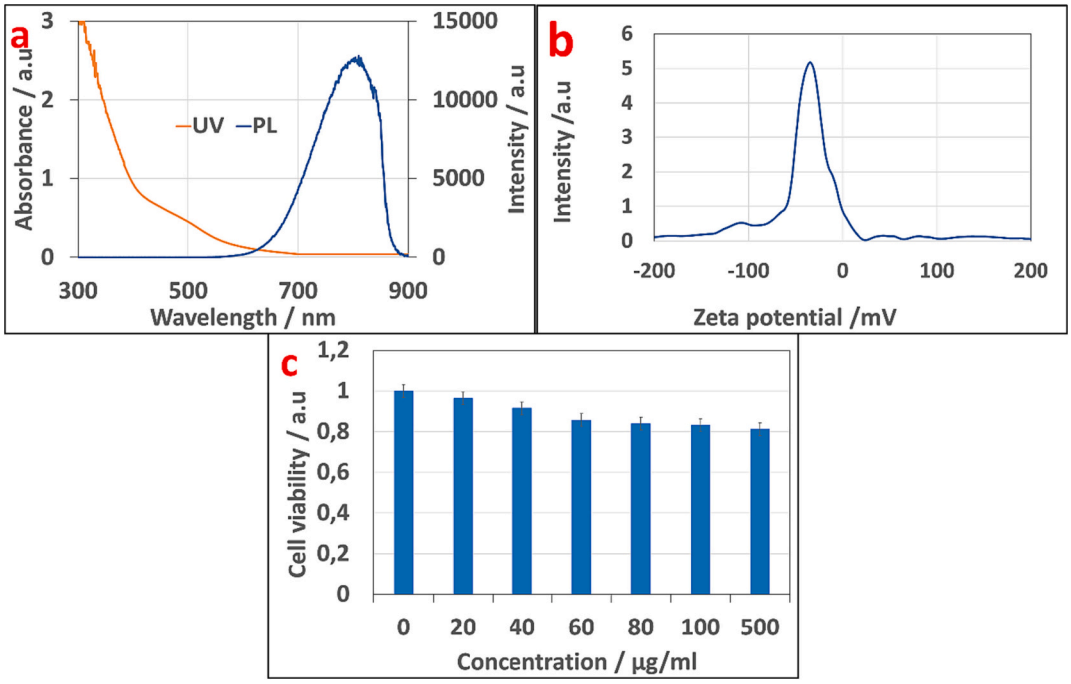

Fig. 1. (a) absorption and emission spectra, (b) zeta-potential and (c) colon cancer cell viability of as-synthesised CISe/ZnS QDs.

to sensing, water purification, and device fabrication, to mention a few [11,12]. Though they have been used extensively in biological applications such as drug delivery, biolabeling, photothermal therapy, photodynamic therapy etc. however, as far as the authors know, their biochemical properties as enzyme inhibitors have not been investigated. We herein report the synthesis of CISe/ZnS QDs and its effect on the activity of furin, a proprotein convertase. The result showed CISe/ZnS QDs as a potent inhibitor of furin with an inhibition constant (K_i) of 15.66 µM. This work is believed to open a niche area in QDs applications, especially as enzymatic inhibitors in drug development against COVID-19 and other emerging diseases.

2. Methodology

2.1. Materials

Copper chloride ($CuCl_2$), indium acetate ($In(C_2H_3O_2)_3$), sodium selenite (Na_2SeO_3), thioglycolic acid (TGA), ammonium hydroxide (NH_4OH), sodium borohydride ($NaBH_4$), tri-sodium citrate (CT), zinc acetate dihydrate ($ZnC_6H_6O_4$), thiourea were purchased from Sigma Aldrich (South Africa). Phosphate-buffered saline (PBS) and Roswell Park Memorial Institute (RPMI) were purchased from Sigma Aldrich (St. Louis, MO, USA). Penicillin and Streptomycin were procured from Life Technologies (Carlsbad, CA, USA). Fetal bovine serum (FBS) was bought from Thermo Scientific (Waltham, MA, USA). Tryptone Soy Broth (TSB) was obtained from Oxoid (Thebarton, Australia). Recombinant soluble human furin was purchased from PeproTech (Rocky Hill, NJ, USA). Fluorogenic furin substrate- pyroglutamic acid-Arg-Thr-Lys-Arg-methylcoumaryl-7-amide (Pyr-RTKR-AMC) was obtained from Calbiochem EMD Millipore Corp. (Billerica, MA, United States). HEPES (4-(2-hydroxyethyl)-1-piperazineethanesulfonic acid) was a product of Sigma-Aldrich Chemical, St. Louis, USA.

2.2. Methods

2.2.1. Synthesis of copper indium selenide-zinc sulfide quantum dot (CISe-ZnS QDs)

The CISe/ZnS QDs were prepared following our reported method for synthesizing AgInSe/ZnS and CISe/ZnS QDs [9,13] with slight modifications. The reaction was carried out in a 4 L pressure cooker with Cu:In:Se mole ratio of 1:4:5. In a typical reaction, 0.77 mmol of CuCl was dissolved in 1500 mL of deionised water under stirring. In a separate beaker 3.08 mmole indium acetate, 3.2 mL thioglycolic acid, and 3 mL ammonium hydroxide were mixed before being transferred to the pressure cooker. This was followed by the addition of 25.1132 g sodium tri-citrate, 0.6646 g sodium selenite and 0.3050 g sodium borohydride, each dissolved in 20 mL of water before being added to the pressure cooker. The solution in the pressure cooker was heated to 120 °C and maintained for 1.5 h to produce CISe core QDs. The solution was cooled naturally to 80 °C followed by the addition of 3.85 mmol (0.8439 g) of zinc acetate and 3.85 mmol (0.2937 g) of thiourea (Zn and S precursors) to grow the shell. The reaction was continued for another 1 h to produce CISe/ZnS QDs. The QDs were precipitated, centrifuged, washed with ethanol, and dried at ambient conditions. The as-synthesised QDs was characterized using the ultraviolet–visible (UV–Vis) and photoluminescence (PL) spectrophotometer, lifetime fluorescence spectroscopy, Fourier-transformed infrared spectroscopy (FTIR), x-ray photon spectroscopy (XPS), energy dispersive spectroscopy (EDS), Zeta potential analyzer and high-resolution transmission electron microscope (HRTEM).

2.2.2. Cell viability

The mouse colon carcinoma cell (C26) was used for toxicological studies of the as-synthesised CISe/ZnS QDS using the previously reported MTT (3-(4,5-dimethylthiazol-2-yl)-2,5-diphenyltetrazolium bromide) assay protocol [9]. The cells were cultured in RPMI enriched with 10% FBS 100 U/mL penicillin and 100 mg/mL streptomycin and incubated at 37 °C in a CO_2 incubator for 48 h to obtain the required confluence and then seeded at the concentration of 1×10^4 cells/mL in a 96-well plate followed by impregnation of each well with different QDs concentrations (0–500 µg/mL) and incubation for 24 h before the addition of 10 µL of MTT solution. The solution was incubated for another 1 h, and its absorbance was measured using a microplate absorbance reader. All the experiments were done in triplicate ($n = 3$) for the reliability of the results, the absorbance values were converted to the % survival ratio of the treated cells with respect to the control.

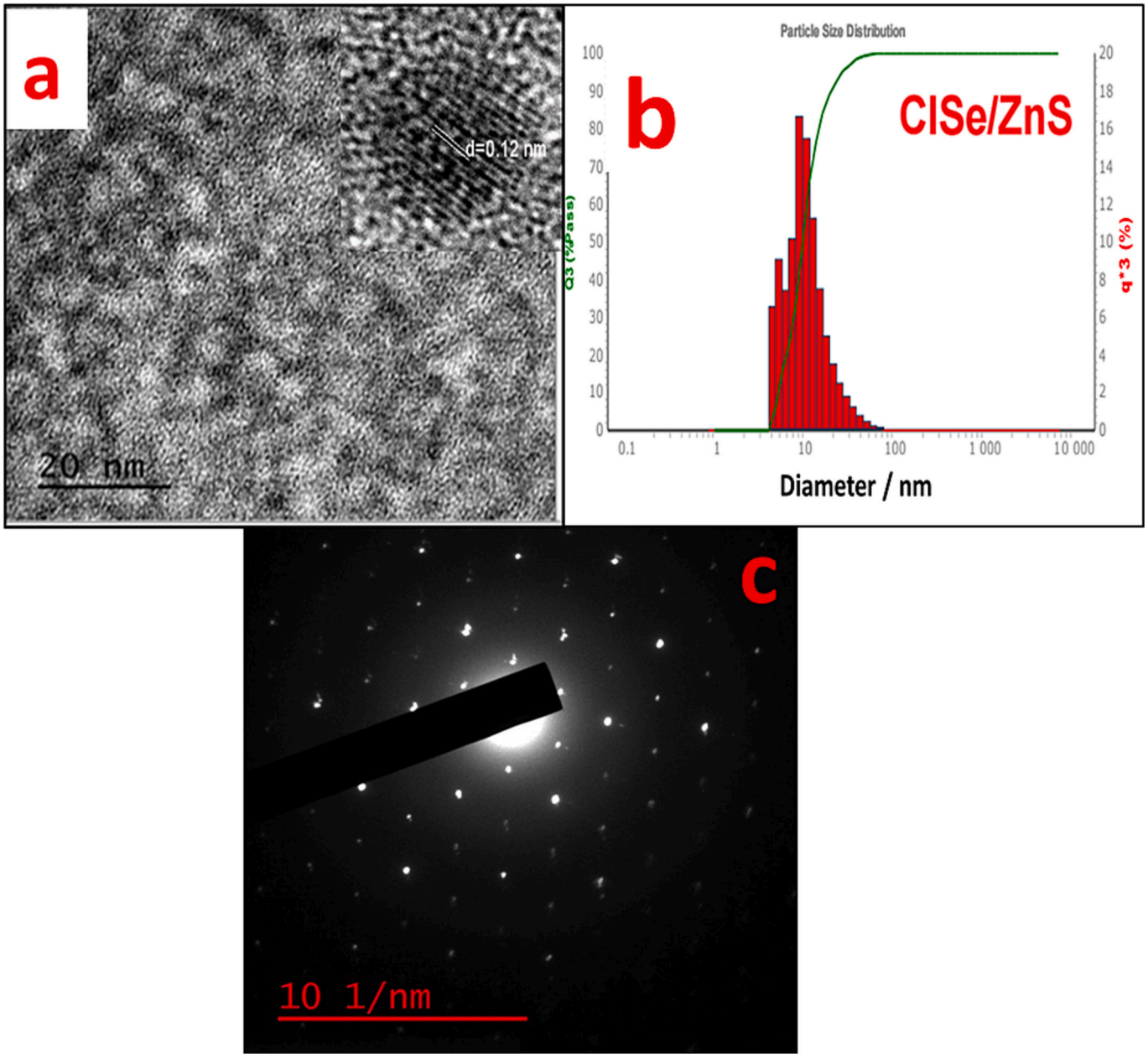

Fig. 2. (a) TEM image: inset-HRTEM, (b) DLS particle size distribution and (c) SAED pattern of the as-synthesised CISe/ZnS QDs.

2.2.3. Furin activity assay

Furin activity assay was carried out following the method of Majumdar et al. (2010) [14] using pyroglutamic acid-Arg-Thr-Lys-Arg-methyl-coumaryl-7-amide (Pyr-RTKR-AMC) as substrate. The recombinant human furin was dissolved in 100 mM HEPES pH 7.0 containing 1 mM $CaCl_2$ and 1 mM 2-mercaptoethanol to form a 5 μg/mL solution. The stock solution of the substrate (200 μM) was prepared in 1% DMSO. An aliquot of 16 μL of 5 μg/mL of furin was loaded into a 96-well plate, and the reaction was started by adding 10 μL of 200 μM substrate in a 40 μL total assay mixture. The fluorogenic 7-amino-4-methyl coumarin (AMC) released per minute in the assay mixture by the enzyme was monitored at excitation and emission wavelengths of 360 nm and 460 nm, respectively, in a fluorescence multi-well plate reader (Applied Biosystems, Inc. USA) at 5 min interval for 60 min. The amount of AMC released per well was estimated from the AMC standard curve prepared.

One unit of furin is defined as the amount of enzyme that will release 1 pmol of AMC from the fluorogenic peptide substrate in one minute (1 pmol of AMC/min) at 30 °C [13].

2.2.4. Effect of substrate concentration on furin activity and determination of kinetic parameters

The effect of substrate concentration on recombinant human (Rh) furin was carried out by measuring initial velocity at varying concentrations of Pyr-RTKR-AMC (0–100 μM). The amount of the fluorogenic AMC released per minute in the assay mixture by the enzyme was monitored as earlier described. Data obtained were analyzed using a non-linear regression curve to determine the enzyme's kinetic parameters- K_m and V_{max} using GraphPad Prism 7 (GraphPad Software Inc., San Diego, CA).

2.2.5. Effect of varying concentrations of CISe/ZnS QDs on furin activity

The effect of CISe/ZnS QDs on furin activity was carried out by assaying for enzyme activity in the absence and presence of CISe/ZnS QDs. Briefly, in the final concentration, the assay mixture (40 μL)

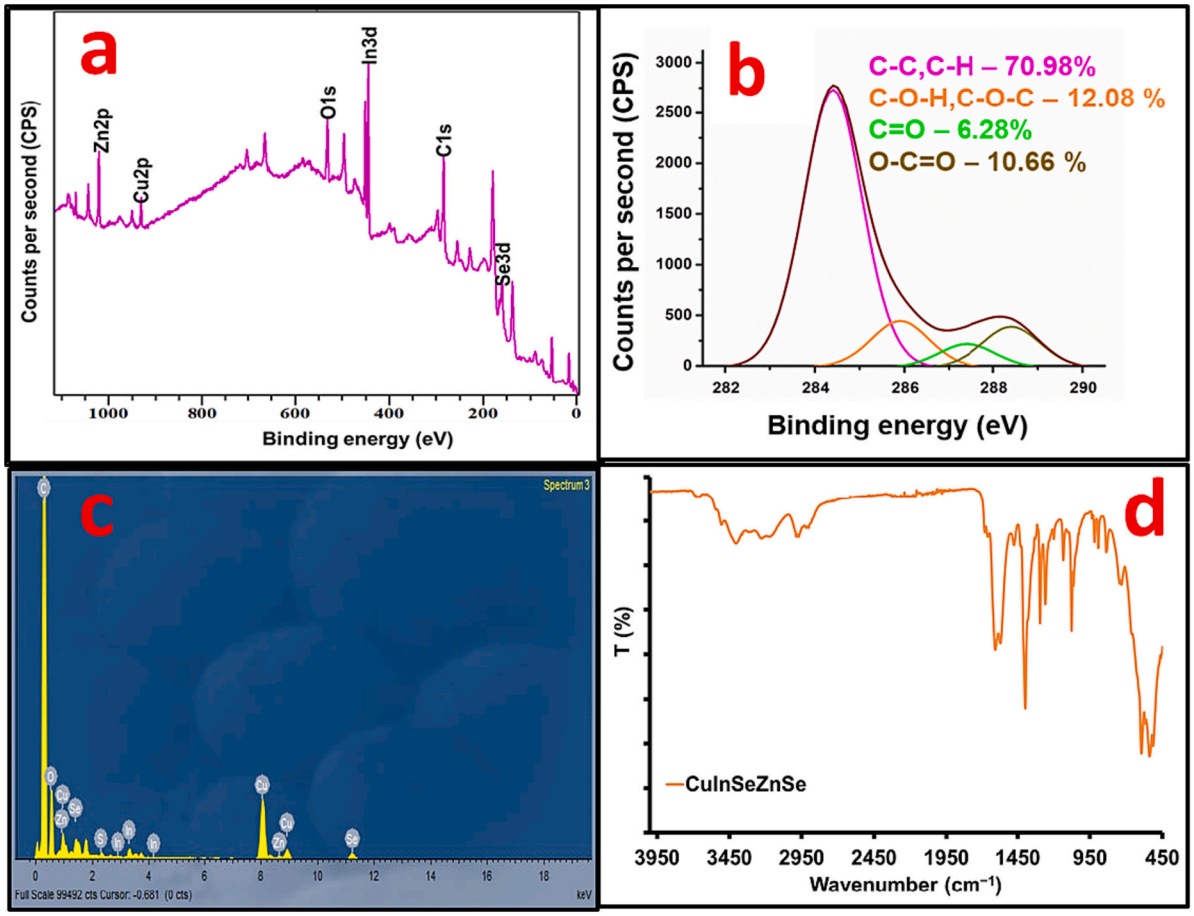

Fig. 3. (a) XPS survey, (b) C1 spectra (c) EDX spectra and (d) FTIR spectra of TGA-Citrate capped CISe /ZnS QDs.

contained 50 μM substrate, 0.08 μg Rh furin and varying concentrations (0–7 μg/mL) of CISe/ZnS QDs. The release of AMC liberated from the substrate was measured at 5 min intervals for 60 min, as stated in section 2.4. The data obtained were used to plot a reciprocal of initial velocity against inhibitor concentration (Dixon plot).

2.2.6. Determination of inhibition constant (Ki) of CISe/ZnS QDs

The inhibition constant of CISe/ZnS QDs for recombinant human (Rh) furin was determined by measuring initial velocity at different fixed substrate concentrations in the absence of the inhibitor and a fixed concentration of the inhibitor. The reciprocal of initial velocity was plotted against the reciprocal of substrate concentrations (Lineweaver-Burk plot).

3. Results and discussions

3.1. Properties of CISe/ZnS QDs

The near-infrared emitting CISe/ZnS QDs was synthesised in a pressure cooker in an aqueous medium via a hydrothermal method with thioglycolic acid and sodium citrate as dual stabilizers. The absorption spectra (Fig. 1a) show an absorption shoulder at 507 nm and an absorption onset at around 619 nm indicating quantum confinement with a maximum emission peak at 820 nm ($\lambda_{500\ nm}$), which is red-shifted from the absorption onset. The as-synthesised QDs showed good stability in aqueous media with a zeta potential of −34.38 mV (Fig. 1b), fluorescence quantum yield of 31% and average lifetime of 24.49 ns. The cell viability analysis against the colon cancer cell line (Fig. 1c) confirmed the excellent biocompatibility of the QDs, even at high concentrations (500 μg/mL), making them suitable for biological studies. The TEM micrograph shows the QDs are nearly spherical and highly crystalline (Fig. 2a). The HRTEM shows the presence of lattice fringes which further confirm the crystallinity of the as-synthesised QDs with a d-spacing of 0.12 nm corresponding to 112 plane of chalcopyrite tetragonal structure. The DLS spectrum shows the hydrodynamic size to be 9.83 nm which is very close to the particle size obtained (6.8 nm) from the TEM. The SAED (Fig. 2c) shows bright diffraction spots indicating the single crystalline nature of the as-synthesised QDs. The XRD pattern provided using the d-spacing in the SAED diffraction pattern shows d-spacing at 0.12 nm, 0.14 nm and 0.24 nm corresponding to (112), (220) and (116) crystalline plane of chalcopyrite tetragonal structure.

The XPS and the EDX were used to investigate the elemental composition while FTIR was used to investigate the surface chemistry of the as-synthesised QDs. The XPS survey spectrum (Fig. 3a) and EDX spectrum (Fig. 3c) show the presence of Zn, Cu, In, Se, S, O and C confirming the elemental composition of the QDs. The functional groups of sodium citrate and thioglycolic acid were confirmed by the high-resolution C1s spectra (Fig. 3b) with a high percentage (70.98%) being C—C and C—H while the rest belonged to their carboxyl groups, constituting the remaining 29.02%. FTIR spectrum of TGA-citrate stabilized CISe/ZnS QDs (Fig. 3d) showed no indication of the S—H TGA peak at 2559 cm^{-1}. This indicates interaction between the TGA thiol group and dangling bonds of CISe/ZnS QDs. The presence of the COO- stretch at 1568 cm^{-1} and O—H bending at 1296 cm^{-1} of the carboxylic group, as well as the C—H stretch and bending at 2972 cm^{-1} and 823 cm^{-1} respectively further confirmed the passivation of the QDs by TGA-citrate dual stabilization. Thus, the QDs has been adequately capped and stable for over 6 months under normal conditions.

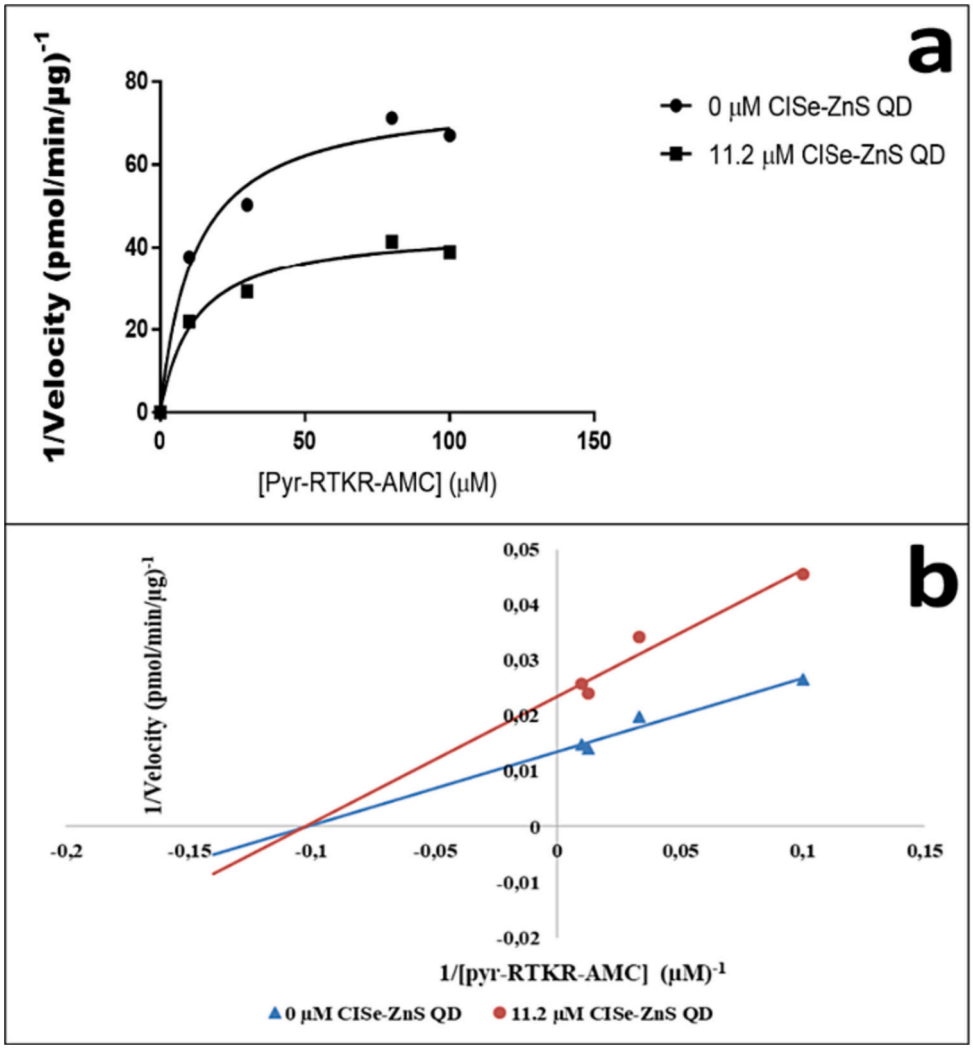

Fig. 4. Effect of substrate concentration on the activity of furin (a) non-linear regression plot of velocity against substrate concentration in the absence of inhibitor and the presence of 11.2 µM of inhibitor (b) Lineweaver-Burk plot of inverse of velocity against the inverse of substrate concentration in the absence of inhibitor and the presence of 11.2 µM of inhibitor.

Table 1
Kinetic parameter of furin in the presence and absence of copper indium selenide- zinc sulphide quantum dot as an inhibitor (I).

Parameter	[I] = 0	[I] = 11.2 µM
K_m	10.79 ± 1.1 µM	10.79 ± 1.1 µM
V_{max}	74.9 ± 1.94 pmol/min/µg	43.66 ± 1.06 pmol/min/µg
K_{cat}	0.08 ± 0.0021 s^{-1}	0.047 ± 0.0011 s^{-1}
K_{cat}/K_m	7.4 × 10^3 ± 0.19 M^{-1} s^{-1}	4.31 ± 0.105 × 10^3 M^{-1} s^{-1}
K_i		15.66 ± 0.75 µM
IC_{50}		11.29 ± 0.54 µM

3.2. Effect of substrate concentration on furin activity

Under our assay condition, an increase in substrate concentration leads to a corresponding increase in initial velocity, and the non-linear regression plot of initial velocity against substrate concentration showed a normal hyperbolic curve (Fig. 4a) with a K_m and V_{max} of 10.79 ± 1.1 µM and 74.9 ± 1.94 pmol/min/µg, respectively. A straight-line curve was obtained in the double reciprocal plot (Fig. 4b). The turnover number (K_{cat}) was 0.08 s^{-1}, and the catalytic efficiency (K_{cat}/K_m) was estimated to be 7.4 × 10^3 M^{-1} s^{-1} (Table 1). In the presence of the QDs as an inhibitor, the Lineweaver-Burk plot intersects on the x-axis (Fig. 4b), suggesting that the inhibition is non-competitive with an inhibition constant (K_i) of 15.66 µM (Table 1). This implies that the enzyme binds the inhibitor at a site other than the active site of the enzyme, which has been reported to contain acidic amino acid residues [16]. The active site of furin is negatively charged; almost all of its substrate must contain basic amino residues [16]. So, it is highly unlikely that CISe/ZnS QDs will have a complementary binding site to such an active site, hence the observed non-competitive inhibition. Further evidence of non-competitive inhibition is that the K_m remains the same in the absence of the inhibitor, but the V_{max} was reduced. The turnover number of furin (K_{cat}), of 0.08 s^{-1} was reduced by half leading to a reduction in the kinetic efficiency of the enzyme (K_{cat}/K_m) by the same magnitude (Table 1).

3.3. Effect of CISe/ZnS QDs on furin activity

An increase in inhibitor concentration led to a corresponding reduction in furin enzymatic activity up to 23 µM when the enzyme activity was totally abolished (Fig. 5a). The concentration of inhibitor at which 50% of the enzymatic activity had been lost (IC_{50}) was 11.29 µM. When the reciprocal of the velocity was plotted against inhibitor concentration (Dixon plot), a non-linear curve (Fig. 5b) was obtained, similar to the behaviour of fatty acyl peptidic inhibitors 10 and 11 of Becker et al. (2012) [16]. The reason for this may be related to the

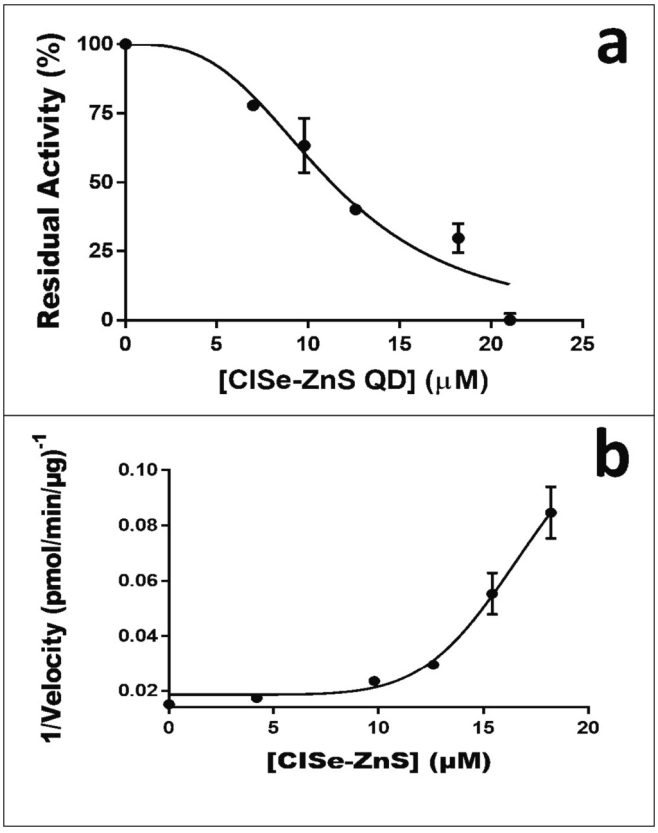

Fig. 5. Inhibition of furin activity by CISe/ZnS QDs using Pyr-RTKR-AMC as fluorogenic substrate (a) Plot of residual furin activity against inhibitor concentration for IC_{50} determination. The substrate concentration was 50 μM. (b) Dixon plot for K_i determination at different concentrations of CISe/ZnS QDs showing non-linearity.

structural change as a result of the binding of the inhibitor to the enzyme; however, further investigation is required to get clarity on this. The K_i of the inhibitor is 15.66 μM placing it as a moderate inhibitor of furin. Compared to some selected inhibitors of furin (Table 2), it has the advantage of low molecular weight and is non-peptidic. Peptide and protein inhibitors or their analogues have problems of toxicity, immunogenicity, instability and low cell permeability [17]. In the case of viral infectious diseases where furin is implicated, e.g. COVID-19, the use of a specific inhibitor targeting the host enzyme rather than targets on the vector would address frequent emergence of drug resistance as a result of a mutation that is part of viral physiology and biochemistry.

4. Conclusion

In summary, we report a facile large-scale synthesis of CISe/ZnS QDs in a cooking pressure cooker and investigate its activity as a potent inhibitor of recombinant human furin, an enzyme that has been implicated in the aetiology of many diseases, including coronavirus (COVID-19). The as-synthesised CISe/ ZnS QDs are small, spherical, highly stable with emission in the near-infrared region (840 nm) and displayed excellent cell viability even at high concentrations. The enzymatic assays showed the QDs as a potent furin inhibitor with an inhibition constant, K_i, of 15.66 μM and (IC_{50}) of 11.29 μM. The turnover number of furin (K_{cat}), was reduced by half leading to a large reduction in the kinetic efficiency of the enzyme (K_{cat}/K_m). The binding of CISe-ZnS QDs to furin was non-competitive, and the enzyme activity was totally abolished at 23 μM inhibitor (CISe/ZnS QDs) concentration. These results indicate the chemotherapeutic potential of CISe/ZnS QDs as an enzyme inhibitor. We believe this will open a niche area in the application of QDs in disease management, particularly as inhibitors of enzymes like furin.

Table 2
Inhibition constants (K_i) of some previously reported furin inhibitors.

Inhibitor	Molecular weight (g/mol)	K_i (μM)	Reference
4- (guanidinomethyl) phenylacetyl-Arg-Tle-Arg-4-amidinobenzylamide	763.9	5.5×10^{-6}	[18]
3-(guanidinomethyl) phenylacetyl-Arg-Val-Arg-4-amidinobenzylamide	749.46	8×10^{-6}	[16]
4-(guanidinomethyl) phenylacetyl-Arg-Val-Arg-4-amidinobenzylamide	749.46	1.6×10^{-5}	[16]
Phenylacetyl-arg-Val-Arg-4-amidinobenzylamide	678.8	0.00081	[6]
Nona-D-arginine	1423.7	0.0013	[19]
Decanoyl-Arg-Val-Lys-Arg-CMK	744.41	0.001	[15]
Phenylacetyl-Arg-Val-Arg-4-amidinobenzylamide	678.8	0.0367	[20]
Acetyl-Val-Arg-4-Amidinobenzylamide	446.3	2.39	[20]
Guanylhydrazones		>3	[23]
Biotin-Adoa-Val-Arg-4-Amidinobenzylamide	929.5	4.2	[20]
Oroxylin A	284.26	5.00 ± 0.04	[14]
*Copper indium selenide-zinc sulfide quantum dots	356.78	15.66 ± 0.75	This report
Baicalein	270.24	26.75 ± 0.95	[14]
Chrysin	254.24	34.91 ± 0.15	[14]
Guanidinylated mono aryl substituted 2,5-dideoxystreptamine derivative		>100	[21]
Andrographolide from *Andrographis paniculata*	350.4	200	[22]

* Inhibitor used in this study.

Funding

This work was carried out under the COVID-19 Africa Rapid Grant Fund supported under the auspices of the Science Granting Councils Initiative in Sub-Saharan Africa (SGCI) and administered by South Africa's National Research Foundation (NRF) in collaboration with Canada's International Development Research Centre (IDRC), the Swedish International Development Cooperation Agency (Sida), South Africa's Department of Science and Innovation (DSI), the Fonds de Recherche du Quebec (FRQ), the United Kingdom's Department of International Development (DFID), United Kingdom Research and Innovation (UKRI) through the Newton Fund, and the SGCI participating councils across 15 countries in sub-Saharan Africa. The authors also thank the National Research Foundation (NRF) under the Competitive Programme for Rated Researchers (CPRR), grant no 129290, Equipment-Related Travel and Training Grants (ERTTG) (Grant No. 129803 and 183560), the University of Johannesburg research committee (URC) and the Faculty of Science research committee (FRC) for financial support.

CRediT authorship contribution statement

Vuyelwa Ncapayi: Investigation, Formal analysis, Validation, Writing – original draft. **Oladoyin Famutimi:** Investigation, Formal analysis, Validation, Writing – original draft. **Thabang Calvin Lebepe:** Validation, Writing – review & editing. **Rodney Maluleke:** Validation, Formal analysis. **Sam Masha:** Validation, Formal analysis. **Nande Mgedle:** Validation, Formal analysis. **Sundararajan Parani:** Validation, Visualization. **Tetsuya Kodama:** Supervision, Resources. **Isaac**

Olusanjo Adewale: Conceptualization, Project administration, Supervision, Funding acquisition, Resources, Writing – review & editing. **Oluwatobi Samuel Oluwafemi:** Conceptualization, Project administration, Supervision, Funding acquisition, Resources, Writing – review & editing.

Declaration of Competing Interest

The authors declare that they have no known competing financial interests or personal relationships that could have appeared to influence the work reported in this paper.

Data availability

Data will be made available on request.

Acknowledgements

The authors thank the National Research Foundation (NRF), South Africa, the University of Johannesburg research committee (URC) and the Faculty of Science research committee (FRC), and Obafemi Awolowo University, Ile -Ife, Nigeria, for providing conducive environments for the project.

References

[1] M. Rose, et al., The role of proprotein convertases in the regulation of the function of immune cells in the oncoimmune response, Front. Immunol. 12 (2021), 667850.
[2] E. Mehranzadeh, et al., What are the roles of Proprotein convertases in the immune escape of tumors? Biomedicines 10 (12) (2022) 3292.
[3] H. Turpeinen, Z. Ortutay, M. Pesu, Genetics of the first seven proprotein convertase enzymes in health and disease, Curr. Genom. 14 (7) (2013) 453.
[4] E. Braun, D. Sauter, Furin-mediated protein processing in infectious diseases and cancer, Clin. Transl. Immunol. 8 (8) (2019) e1073.
[5] J. Shang, et al., Cell entry mechanisms of SARS-CoV-2, Proc. Natl. Acad. Sci. 117 (21) (2020) 11727.
[6] G.L. Becker, et al., Potent inhibitors of Furin and Furin-like proprotein convertases containing decarboxylated P1 arginine mimetics, J. Med. Chem. 53 (3) (2010) 1067.
[7] O.S. Oluwafemi, et al., Facile, large scale synthesis of water soluble AgInSe2/ZnSe quantum dots and its cell viability assessment on different cell lines, Mater. Sci. Eng. C 106 (2020), 110181.
[8] N. Zikalala, S. Parani, O.S. Oluwafemi, Aqueous synthesis of Zn-based ternary core/shell quantum dots with excellent stability and biocompatibility against different cell lines, J. Mater. Sci. 57 (12) (2022) 6780.
[9] V. Ncapayi, et al., Diagnosis of prostate cancer and prostatitis using near infra-red fluorescent aginse/zns quantum dots, Int. J. Mol. Sci. 22 (22) (2021) 12514.
[10] I. Yakavets, et al., NIR imaging of the integrin-rich head and neck squamous cell carcinoma using ternary copper indium selenide/zinc sulfide-based quantum dots, Cancers 12 (12) (2020) 3727.
[11] B. Poornaprakash, et al., *Enhanced fluorescence efficiency and photocatalytic activity of ZnS quantum dots through Ga doping*, Ceram. Int. 45 (2) (2019) 2289.
[12] B. Poornaprakash, et al., Terbium-doped ZnS quantum dots: structural, morphological, optical, photoluminescence, and photocatalytic properties, Ceram. Int. 44 (10) (2023) 11724.
[13] N. Tsolekile, et al., Synthesis of fluorescent CuInS2/ZnS quantum dots—porphyrin conjugates for photodynamic therapy, MRS Commun. 8 (2) (2018) 398.
[14] S. Majumdar, et al., Proprotein convertase inhibitory activities of flavonoids isolated from Oroxylum indicum, Curr. Med. Chem. 17 (19) (2010) 2049.
[15] A.G. Remacle, et al., Selective and potent furin inhibitors protect cells from anthrax without significant toxicity, Int. J. Biochem. Cell Biol. 42 (6) (2010) 987.
[16] G.L. Becker, et al., Highly potent inhibitors of proprotein convertase furin as potential drugs for treatment of infectious diseases, J. Biol. Chem. 287 (26) (2012) 21992.
[17] T. Osadchuk, O. Shybyryn, V. Kibirev, Chemical structure and properties of low-molecular furin inhibitors, Ukr. Biochem. J. 88 (6) (2016) 5.
[18] K. Hardes, et al., Novel furin inhibitors with potent anti-infectious activity, ChemMedChem 10 (7) (2015) 1218.
[19] M.M. Kacprzak, et al., Inhibition of furin by polyarginine-containing peptides: nanomolar inhibition by nona-D-arginine, J. Biol. Chem. 279 (35) (2004) 36788.
[20] M. Kuester, et al., Purification of the proprotein convertase furin by affinity chromatography based on PC-specific inhibitors, 2011, p. 973.
[21] G.-S. Jiao, et al., Synthetic small molecule furin inhibitors derived from 2, 5-dideoxystreptamine, Proc. Natl. Acad. Sci. 103 (52) (2006) 19707.
[22] A. Basak, et al., Inhibition of proprotein convertases-1,-7 and furin by diterpines of Andrographis paniculata and their succinoyl esters, Biochem. J. 338 (1) (1999) 107.
[23] S.O. Dahms, et al., OFF-state-specific inhibition of the proprotein convertase furin, ACS Chem. Biol. 16 (9) (2021) 1692.